Chinese Journal of Oceanology and Limnology

http://dx.doi.org/10.1007/s00343-014-3150-2

Characterization of calcium deposition induced by *Synechocystis* sp. PCC6803 in BG11 culture medium*

YAN Huaxiao (闫华晓)[1], HAN Zuozhen (韩作振)[2, 3, **], ZHAO Hui (赵辉)[1, 2], ZHOU Shixue (周仕学)[1, **], CHI Naijie (迟乃杰)[2], HAN Mei (韩梅)[2], KOU Xiaoyan (寇小燕)[1], ZHANG Yan (张艳)[1], XU Linlin (徐琳琳)[1], TIAN Chenchen (田晨晨)[1], QIN Song (秦松)[4]

[1] *College of Chemical and Environmental Engineering, Shandong University of Science and Technology, Qingdao 266590, China*

[2] *Shandong Provincial Key Laboratory of Depositional Mineralization and Sedimentary Minerals, College of Geological Science and Engineering, Shandong University of Science and Technology, Qingdao 266590, China*

[3] *State Key Laboratory of Mining Disaster Prevention and Control, Shandong University of Science & Technology, Qingdao 266590, China*

[4] *Yantai Institute of Coastal Zone Research, Chinese Academy of Sciences, Yantai 264003, China*

Received May 6, 2013; accepted in principle Jun. 25, 2013; accepted for publication Jul. 26, 2013

Abstract Calcium carbonate ($CaCO_3$) crystals in their preferred orientation were obtained in BG11 culture media inoculated with *Synechocystis* sp. PCC6803 (inoculated BG11). In this study, the features of calcium carbonate deposition were investigated. Inoculated BG11 in different calcium ion concentrations was used for the experimental group, while the BG11 culture medium was used for the control group. The surface morphologies of the calcium carbonate deposits in the experimental and control groups were determined by scanning and transmission electron microscopy. The deposits were analyzed by electronic probe micro-analysis, Fourier transform infrared spectrum, X-ray diffraction, thermal gravimetric analysis and differential scanning calorimetry. The results show that the surfaces of the crystals in the experimental group were hexahedral in a scaly pattern. The particle sizes were micrometer-sized and larger than those in the control group. The deposits of the control group contained calcium (Ca), carbon (C), oxygen (O), phosphorus (P), iron (Fe), copper (Cu), zinc (Zn), and other elements. The deposits in the experimental group contained Ca, C, and O only. The deposits of both groups contained calcite. The thermal decomposition temperature of the deposits in the control group was lower than those in the experimental group. It showed that the $CaCO_3$ deposits of the experimental group had higher thermal stability than those of the control group. This may be due to the secondary metabolites produced by the algae cells, which affect the carbonate crystal structure and result in a close-packed structure. The algae cells that remained after thermal weight loss were heavier in higher calcium concentrations in BG11 culture media. There may be more calcium-containing crystals inside and outside of these cells. These results shall be beneficial for understanding the formation mechanism of carbonate minerals.

Keyword: *Synechocystis* sp. PCC6803; preferred orientation; biomineralization; calcium carbonate; thermal stability

1 INTRODUCTION

Calcium carbonate ($CaCO_3$) is one of the most common bio-minerals in nature, and exists mainly in three anhydrous polymorphs and three hydrated polymorphs (Spanos and Koutsoukos, 1998; Castanier et al., 1999; Ren et al., 2011). The forms are calcium carbonate hexahydrate ($CaCO_3 \cdot 6H_2O$), amorphous calcium carbonate (ACC), and calcium carbonate monohydrate ($CaCO_3 \cdot H_2O$), and the three mineral

* Supported by the National Natural Science Foundation of China (Nos. 40972043, 41040018, 41210104058, 21176145, 41372108, 41302079), the Higher Educational Science and Technology Program of Shandong Province (No. J10LC15), the China Postdoctoral Science Foundation (No. 2013M540560), the Program for Scientific Research Innovation Team in Colleges and Universities of Shandong Province, and SDUST Research Fund (No. 2010KYTD103), the Open Project of Key Lab of Marine Bioactive Substance and Modern Analytical Technique, State Oceanic Administration, China (No. MBSMAT-2012-03), the Scientific and Technological Program of Qingdao (No. 13-1-4-232-jch), and the Domestic Visiting Scholar Program for Young Core Teachers in Shandong Universities, Shandong Province, China
** Corresponding authors: hanzz@163.com; yzsxue@126.com

forms vaterite, aragonite, and calcite, in increasing order of thermodynamic stability (Milliman et al., 1999; Kimura and Koga, 2011; Liu et al., 2013). Vaterite and aragonite nucleate slowly and grow stably in biological systems (Cōlfen, 2003). Their crystal lattices can maintain stability in manmade environments formed by organic molecules, such as amino acids, nucleic acids, and polysaccharides (Fujita et al., 2000; Manoli and Dalas, 2000; Tong et al., 2004). In the past 20 years, many microorganisms have been found to have the ability to precipitate $CaCO_3$ (de Vrind-de Jong and de Vrind, 1997; Hammes and Verstraete, 2002; Cacchio et al., 2003; Hammes et al., 2003; Dittrich et al., 2004; Han et al., 2013). Microbes encourage these processes by increasing the surface area for nucleation (Dittrich et al., 2003), creating alkaline environments near the cell surface (Lee et al., 2006), and increasing the concentrations of dissolved inorganic carbon through their physiological activity (Rippka et al., 1979; Yeager et al., 2011).

The cyanobacterium *Synechocystis* sp. PCC6803 is capable of photosynthetic growth, and is used as a typical organism for the study of oxygenic photosynthesis of plants because it has relatively simple genetic systems. However, there are few concrete studies about the involvement of *S.* sp. PCC6803 in calcium carbonate mineral deposition and sedimentary processes. In this study, *S.* sp. PCC6803 was used as an organic template to induce the nucleation and growth of calcium carbonate. The aim of this paper is to analyze the surface morphology of the calcium carbonate deposit by scanning electron microscopy (SEM) and transmission electron microscopy (TEM), and to characterize the structure and elementary composition of the deposit by electron probe microanalysis (EPMA), Fourier transform infrared (FTIR) spectroscopy, X-ray powder diffraction (XRD), thermo-gravimetric/differential thermal analysis (TG/DTA) and differential scanning calorimetry (DSC).

2 MATERIAL AND METHOD

2.1 Cyanobacteria strain, culture medium, and cultivation conditions

The bacterial strain cyanobacteria *S.* sp. PCC6803 was obtained from the Qingdao Institute of Bioenergy and Bioprocess Technology, Chinese Academy of Sciences. *S.* sp. PCC6803 cells were cultured in modified BG11 liquid culture medium or agar plates. The modified BG11 medium consisted of (per liter) 0.001 g EDTA (disodium salt), 1.5 g $NaNO_3$, 0.006 g ferric ammonium citrate, 0.006 g citric acid, 0.075 g $MgSO_4 \cdot 7H_2O$, 0.04 g K_2HPO_4, 0.02 g Na_2CO_3, 2.9 mg H_3BO_3, 1.8 mg $MnCl_2 \cdot 4H_2O$, 0.22 mg $ZnSO_4 \cdot 7H_2O$, 0.08 mg $CuSO_4 \cdot 5H_2O$, 0.05 mg $Co(NO_3)_2 \cdot 6H_2O$, 0.39 mg $NaMoO_4 \cdot 2H_2O$ and different concentrations of calcium ions. The 100 g/L Ca^{2+} mother liquor preparation method was as follows: 25 g calcium carbonate (Shiyi Chemical Reagent Co., Ltd., Shanghai, China) was placed in a 250-mL beaker, an excess of concentrated hydrochloric acid was added, the solution was transferred to a volumetric flask, and then distilled water was added until the volume was 100 mL. Specific volumes of the 100 g/L Ca^{2+} mother liquor were added to the BG11 medium to make the calcium ion concentrations of the medium 0, 9.8 (calcium ion concentration of the original BG11 medium), 100, 200, 300, 400, 500, 600, 700, 800, 900, and 1 000 mg/L. *S.* sp. PCC6803 cells were cultured in the modified BG11 liquid medium and placed in a light growth chamber GPX-250B. The culture conditions were maintained at 25°C with photon irradiance of 28 μmol/(s·m) and 12 h light/dark cycles.

2.2 Deposit obtained from the modified BG11 medium

The modified BG11 culture medium without inoculation by *S.* sp. PCC6803 cells was used as the control. The control and culture media containing *S.* sp. PCC6803 cells were cultured under the same conditions. The deposit in the control containing 1 000 mg/L Ca^{2+} was obtained by 5 min centrifugation at 15 000 r/min. Then, the deposit at the bottom of centrifugal tube was dried in the oven at 40°C for 24 h.

2.3 Surface morphology analysis of the deposit by SEM and TEM

The deposits were studied by SEM and TEM combined with electron diffraction. The SEM images were taken in a scanning electron microscope (KYKY-2800B). HRTEM measurements were carried out with a transmission electron microscope (JEM-2100).

2.4 Composition and structure analysis of the deposit by EPMA, FTIR, XRD

Elemental analysis of the deposits was carried out using an electronic probe micro analyzer (JEOL JXA-8230) with a linked energy dispersive spectrometer

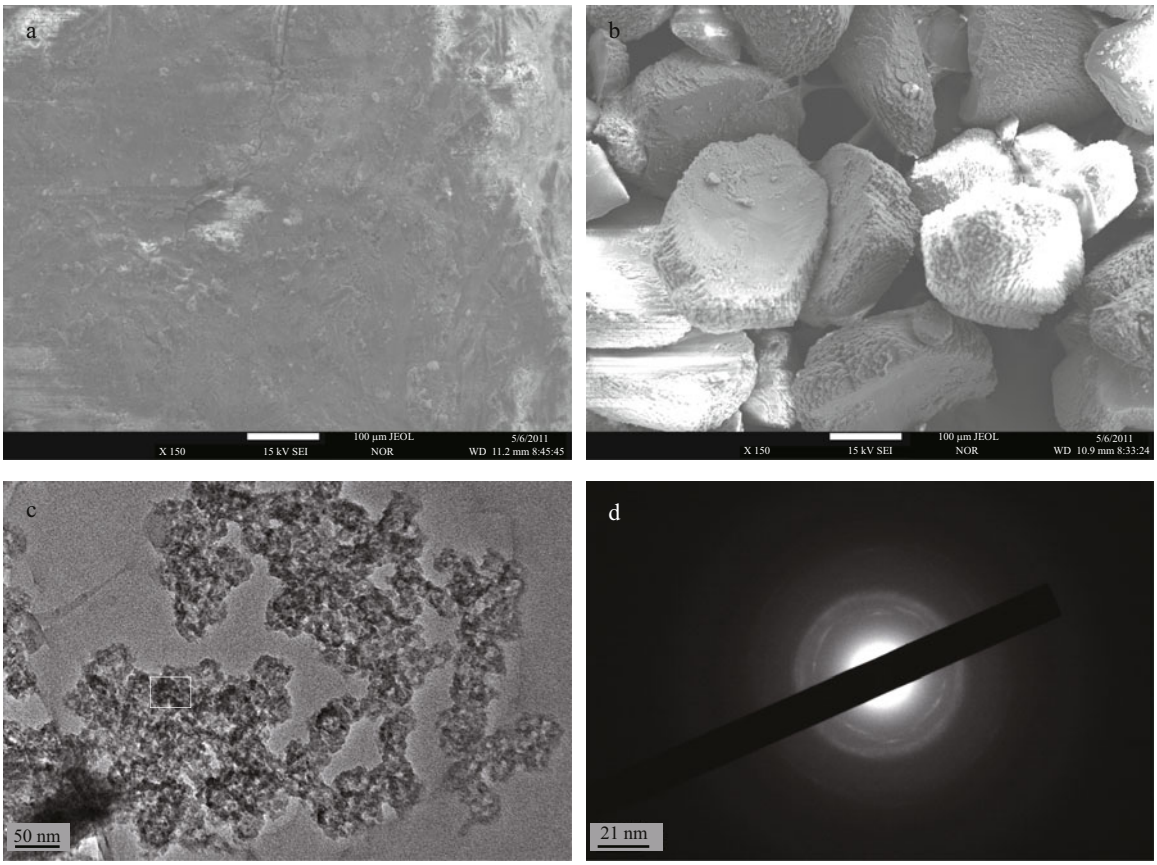

Fig.1 Surface morphology analysis of the deposit by SEM and TEM

a. The surface morphology of deposit generated from the control group by SEM; b. The surface morphology of deposit generated from BG11 medium inoculating with PCC6803 by SEM; c. The surface morphology of deposit generated from the control group by TEM; d. Electron diffraction of the selected area of the deposit generated from the control group, the white square in Fig.1c showed the selected area.

(EDS) (INCA ENERGY350) at 20 KV, 2.4 nA, and a count time of 100 s. FTIR analyses were performed with a FTIR-8400S spectrometer (resolution 4/cm; gain 1; 4 000 to 500/cm; 40 scans). The samples were analyzed by the potassium bromide (KBr) technique. The deposits were analyzed by a D/Max-RC XRD instrument, at a 2θ angle range of 20°–50°, in a step size of 0.02, and a count time of 8°/min.

2.5 Deposit analysis by TG-DTA and DSC

TG-DTA analysis and DSC measurements were carried out using a thermogravimetric analyzer (TGA/DSC1/1600LF, Mettler Toledo Co., Switzerland). The deposits were analyzed in a nitrogen atmosphere (flow rate=100 cm^3/min) at a heating rate of 10°C/min, from room temperature to 950°C. TGA has the capability of measuring the mass loss of the deposit, whereas DTA has the capability of measuring the temperature difference. TGA and DSC measurements were performed to determine changes in the deposit weight, and to investigate the thermal behaviour from physical and chemical changes during the heat treatment.

3 RESULT

3.1 Surface morphology of the deposit by SEM and TEM

The deposit (Fig.1a) produced in the control was composed of nanometer-sized particle. No typical shape of crystals was found in the deposits when they were magnified 150, 500, 1 000, and 2 000 times by SEM. The superfine powders were mixed with a few particles with a size of a few microns. The result indicated that the composition of the deposit in the control was complex and contained small crystals as well as non-crystalline material. The deposit obtained from the BG11 culture medium inoculated with PCC6803 (inoculated BG11) had well-shaped crystals, generally in the shape of hexagons (Fig.1b). The lengths of the particles were about 300 μm and the widths about 150 μm. The surface

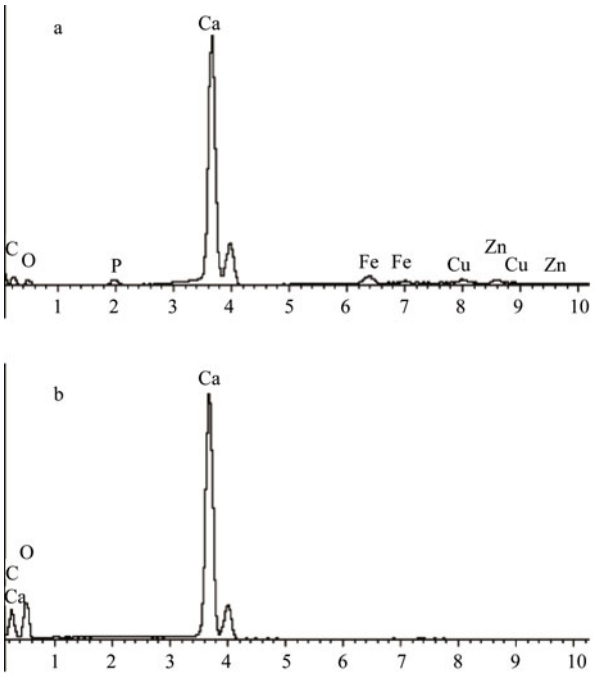

Fig.2 The element composition analysis of the deposit by EPMA

a. Element analysis of deposit generated from the control group by EPMA; b. Element analysis of deposit generated from medium inoculating with PCC6803 by EPMA.

Table 1 Element analysis of deposit from the control by EPMA

Element	Quality ratio (%)	Atomic ratio (%)	Compound ratio (%)	Chemical formula
C	3.10	6.68	11.36	CO_2
P	0.77	0.64	1.77	P_2O_5
Ca	55.33	35.73	77.41	CaO
Fe	6.42	2.97	8.26	FeO
Cu	0.06	0.02	0.08	CuO
Zn	0.01	0.01	0.02	ZnO
I	1.11	0.23	0.00	
O	33.20	53.71		
Total	100.00			

Table 2 Element analysis of the deposit from the medium with inoculation of PCC6803 by EPMA

Element	Quality ratio (%)	Atomic ratio (%)	Compound ratio (%)	Chemical formula
C	7.54	14.06	27.63	CO_2
Ca	51.72	28.90	72.37	CaO
O	40.74	57.03		
Total	100.00			

micromorphology of the deposit was clearly observed using SEM. Each particle was hexahedral with a rough surface, forming a scaly structure. TEM was used to further study the surface of the precipitation particles in the control group. Figure 1c is a representative TEM image of the deposit obtained from the control. In the images, some embedded particles were found. These particles had an average size of a few nanometers. Figure 1d shows that the corresponding diffraction pattern has diffuse haloes, which is evidence for a crystalline structure. The structure of the particles in the deposit from the control group is evident in the diffraction pattern. However, the bulk deposit of the control group has an amorphous structure because there is an absence of any crystalline features. This means that the deposit in the control group contains abundant amorphous particles and a small number of crystalline particles with nanometer size.

3.2 Composition and structure of the deposit by EPMA, FTIR, and XRD analyses

The elemental analysis by EPMA showed that the composition of the deposit from the control was complex, containing calcium (Ca), carbon (C), oxygen (O), phosphorus (P), iron (Fe), copper (Cu), zinc (Zn), as well as other elements (Fig.2a). From Table 1, Ca and O had the largest percentages of 55.33% and 33.20%, respectively, followed by Fe and C.

Figure 2b shows that the deposit produced in inoculated BG11 contained fewer elements than that produced in the control: only Ca, C, and O. Table 2 shows that the ratio Ca:C:O was about 6.86:1:5.40. The ratio of Ca:C:O in $CaCO_3$ is 3.3:1:4, so it can be concluded that $CaCO_3$ was contained in the deposit. This leaves only Ca and O in addition to $CaCO_3$, and the ratio of the two elements Ca:O was 2.54:1. The ratio of Ca and O in CaO is 2.5:1, indicating that Ca and O combined to form CaO in the deposit. Therefore, the deposit produced in inoculated BG11 may contain $CaCO_3$ and CaO. After further analysis by XRD, the deposit was confirmed to contain $CaCO_3$. From the XRD analysis, the deposition contained $CaCO_3$ with good crystallinity and amorphous CaO.

The infrared spectrum of the deposit produced in inoculated BG11 was compared with that obtained from the control. The features of calcite peaks in the control are as follows: CO_3^{2-} asymmetrical stretching vibration peak (V_3) 1 421/cm, CO_3^{2-} plane bending vibration peak (V_2) 877–848/cm, and CO_3^{2-} out-of-plane bending vibration peak (V_4) 712/cm. After

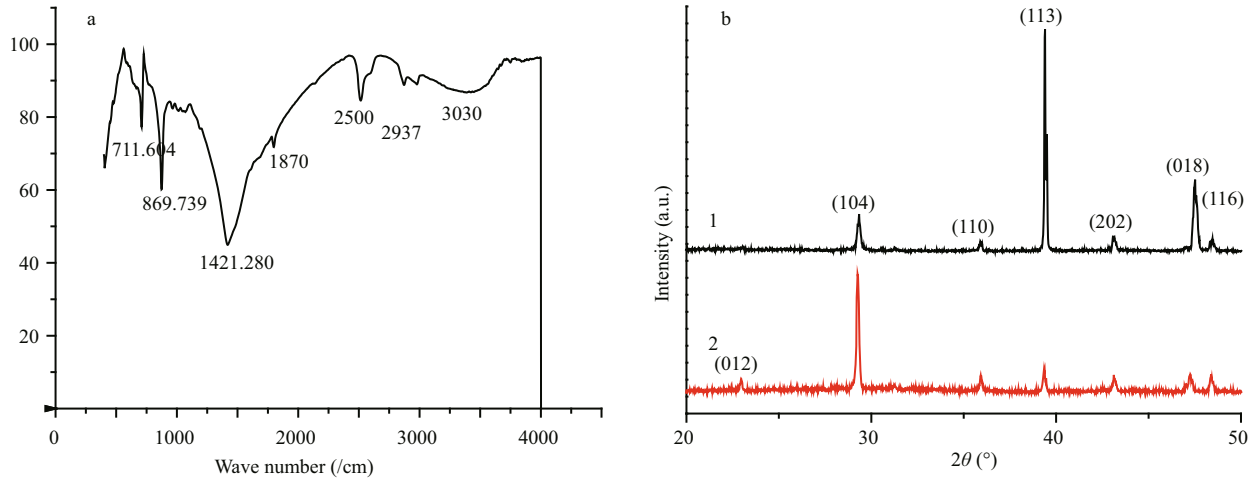

Fig.3 Analysis of the deposit by FTIR and XRD

a. FTIR analysis of deposit generated from medium inoculating with PCC6803; b. X-ray diffraction of deposit: 1. Deposit generated from medium inoculating with PCC6803; 2. Deposit generated from control group.

comparison with the IR spectrum of the control, the crests of the deposit also coincided with those of calcite (Fig.3a). Thus, the deposit produced in inoculated BG11 was confirmed as calcite.

Unsaturated C-H bonds show stretching vibrations at a frequency higher than 3 000/cm. The peak at 3 030/cm in Fig.3a indicates that the compound contains unsaturated C-H bonds. The absorption peaks of unsaturated double bonds (C=C-H) appear in the range 3 010–3 040/cm. The benzene ring (C=CH) bond stretching vibration usually occurs at 3 030/cm. Stretching vibrations of saturated C-H bonds occur from 2 800–3 000/cm, that is, lower than 3 000/cm. Substituents have little effect on the stretching vibrations. The peak at 2 937/cm in Fig.3a indicates that the chemical compound contains saturated C=C-H bonds. The R_2CH_2 group absorption peaks are at about 2 850/cm and 2 930/cm. Peaks of naphthene and -CH_2- connected to a halogen shift to a higher frequency. The absorption peaks of C≡C, C≡N and C=C=C occur between 2 000–2 500/cm. The peak at 2 500/cm in Fig.3a indicates that chemical compound contains C≡C and/or C≡N and/or C=C=C bonds. The C=O stretching vibration appears in the range 1 650–1 900/cm. Carbonyl absorption is usually one of the strongest peaks in the range 1 690–1 760/cm, and groups connected to the carbonyl group will affect the frequency of the absorption peak. The peak at 1 870/cm in Fig.3a indicates that the compound contains C=O bonds.

From the XRD analysis (Fig.3b), there are clear differences between the deposits obtained from inoculated BG11 and the control group. As shown in Fig.3b, samples 1 and 2 are $CaCO_3$ crystals with different crystal orientations. Mainly because of the addition of PCC6803, the calcium carbonate crystals showed preferred orientation growth. The diffraction peak intensity of the crystal planes (012) and (104) decreased, while the intensities of the crystal planes (113(-)), (018) and (1,2,10(-)) increased. This suggests that there is a preferred orientation during the growth of the calcium carbonate crystals when the medium is inoculated with PCC6803. Figure 1b shows that the deposit grew up and a scale-like structure was formed with the inoculated BG11 medium. The scale-like structure indicates that the orders of the crystals' growth were in a given direction and proved the preferred orientation of the crystals' growth (Fig.1b).

3.3 TG-DTA and DSC analysis of the deposition

Figure 4a and b shows that each of these two samples has two weight loss peaks. The first peak of sample 1 indicates that when the deposit from the control was heated the sample started to lose weight to about 100°C. The weight loss at 100°C is due to evaporation of free and crystal water, and the peak from 100–200°C is due to the loss of coordination water. At about 250°C, sample 2 began to lose more weight, which is thought to be due to decomposition of organic and/or oxidation substances. The algae cells were possibly not cleanly eliminated in the separation process of PCC6803 cells and deposition. The second weight loss peak of the two samples was from 600–800°C, suggesting that carbonate may exist in both of the samples. The decomposition temperatures of sample 1 and 2 were 687.3°C and

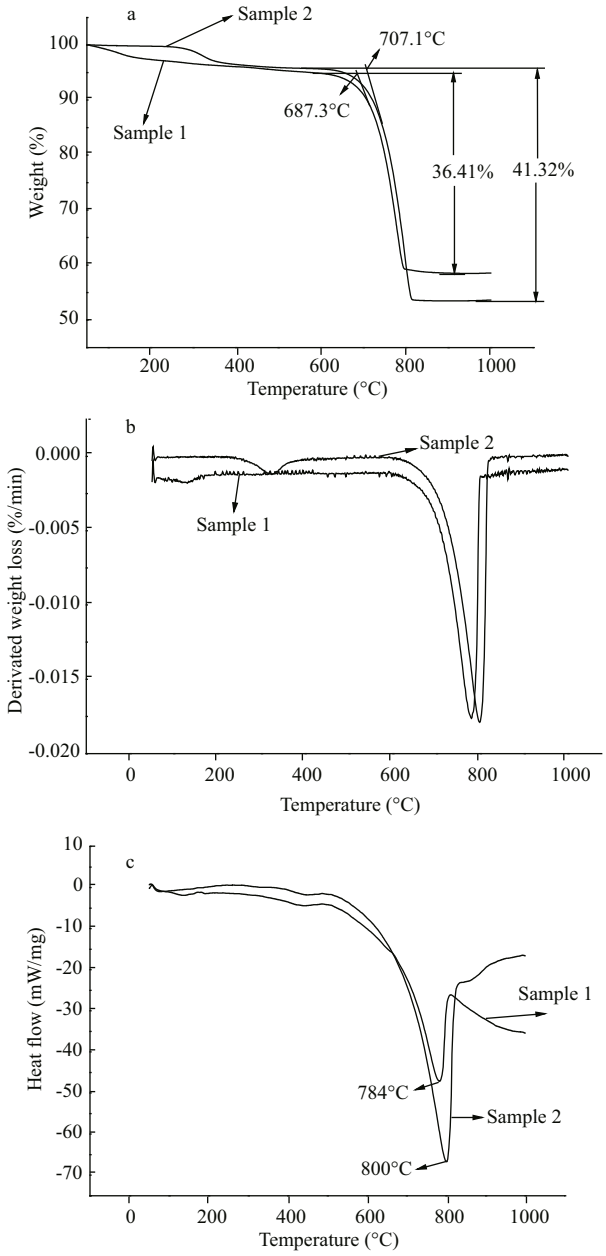

Fig.4 TG, DTG and DSC analysis of the deposit

a. TG analysis; b. DTG analysis; c. DSC analysis. Sample 1. The deposit obtained from the control group; Sample 2. The deposit obtained from the culture media with inoculation of *S.* sp. PCC6803 cells.

707.1°C, respectively, indicating that sample 2 decomposes 20°C higher than sample 1. Therefore, there is a clear difference between the two samples, which is mainly exhibited in their decomposition temperatures. This is probably due to the different crystal structures, particle sizes, and crystal degrees of the two samples. It was estimated that the closer atomic arrangement and more crystalline structure of sample 2 led to the higher decomposition temperature.

After the second weight loss, the weight of sample 1 decreased 36.41% and the remainder was 60%, while the weight of sample 2 decreased 41.32% and the remainder was about 55% (Fig.4a). The breakdown products of $CaCO_3$ were CaO and CO_2, and the quality percentages of CO_2 and CaO in $CaCO_3$ were 44% and 56%. The loss and the quality percentage of sample 2 generally agree with the values for $CaCO_3$, which confirmed sample 2 was $CaCO_3$. However, the crystal structure of sample 2 was different from $CaCO_3$ because there were more remainders in sample 1 than sample 2, indicating that it might contain other substances.

Figure 4c shows that there is a prominent sharp heat absorption peak in the curves of both samples. Such sharp peaks indicate that the two samples have high purity. The temperature of the sharp heat absorption peak of sample 1 is at 784°C and for sample 2 it is at 800°C. XRD analysis showed that in sample 2 the crystal was in the preferred orientation and different from sample 1. Therefore, $CaCO_3$ deposits generated from inoculated BG11 had a higher thermal stability. The existence of elements in the control group, such as Fe, Cu and Zn, may have an effect on the stability of calcium carbonate. The atomic radii of Fe, Cu, and Zn are larger than the atomic radius of Ca. Thus, the interatomic distances in ionic crystals formed by Fe, Cu, and Zn are greater than the interatomic distances in crystals formed by Ca, and the thermal stabilities of these crystals are likely to be lower than those of Ca. There are possibly other reasons. The secondary metabolites produced by algae cells could affect the carbonate crystal structure. These organic molecules interact with calcium ions, and may affect the arrangement of atoms in the carbonate crystal. The atoms are closely packed to shorten the interatomic distances, so crystals formed in this case would have higher thermal stability.

To explore the reasons for the weight loss in sample 2 at about 250°C, algae cells cultured in various concentrations of calcium were used for TG analysis (Fig.5). It was found that the cells lost weight at 250°C (Fig.5). This confirmed that the second weight loss of the deposit (sample 2) at about 250°C was due to the decomposition of organic algae cells. The weight of the algae cells remained after heating at 250°C increased with increasing calcium concentration in the culture environment, which suggests that calcium enters into the *Synechocystis* cells.

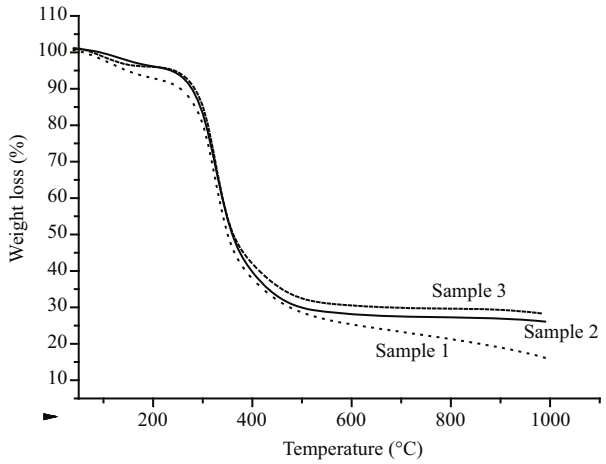

Fig.5 TG analysis of PCC6803 cells cultured in medium with different concentrations of calcium

Sample 1, PCC6803 cells cultured in BG11 medium without additional calcium ions; Sample 2, PCC6803 cells cultured in medium with 500 mg/L calcium ions; Sample 3, PCC6803 cells cultured in medium with 1 000 mg/L calcium ions.

4 DISCUSSION

The deposit obtained from the control was produced by natural precipitation. Natural precipitation refers to when the concentration of Ca^{2+} ions reaches a certain level in the solution then it will bind the CO_3^{2-} ion to form calcium carbonate precipitate. The whole process does not require any external forces. Precipitate by itself occurs only under suitable conditions. In this experiment, the deposit in the control contained calcium carbonate nanometer-sized crystals through physical and chemical effects without auxiliary forces. There are many reasons for the formation of the deposit induced by PCC6803 cells. The PCC6803 cell wall has a reticulated structure and contains a number of negatively-charged functional groups. Transparent colloid is composed of polysaccharide, which is highly viscous and can absorb the calcium carbonate particles suspended in the liquid to the cell surface, resulting in precipitation (Ren et al., 2011). Therefore, the number of sediment particles formed in this type of culture is significantly greater than for the control group. The cell wall surface provides many functional groups that can bind with calcium ions. Most of these groups are amino, carboxyl, hydroxyl, aldehyde, and sulfate groups, and among these the carboxyl group is the most important. For example, two adjacent polymers can join together using two carboxyl groups via a Ca^{2+} bridge. Then, the Ca^{2+} ions attract anions and the anion concentration increases in the local environment, attracting more Ca^{2+} ions. When the concentration increases to a certain level, calcium carbonate heterogeneous nucleation occurs (Liu et al., 2013). When the Ca^{2+} concentration is insufficient for heterogeneous nucleation, organic calcium aggregates outside the cell wall. The carbonate groups produced by post-decomposition of organic matters easily form precipitates of calcium carbonate particles by binding calcium ions. In the process of nucleation, the polysaccharide on the surface of the cell wall plays an important role. When the surface of the cell wall is coated with large calcium carbonate particles, the cells will not be able to photosynthesize, resulting in cell death. The internal functional groups of the dead cells will then be exposed to bind more metal ions. The main internal functional groups are carboxyl (C=O), amine (NH_2), hydroxyl (-OH), and phosphate groups (HPO_4^{2-}). When the cells die, organic matter decomposes and produced a large number of CO_3^{2-} ions, which can combine with calcium ion and form a large amount of calcium carbonate with good crystallinity. Therefore, the resulting structures of the deposits are different according to the different sediment formation mechanisms, and the natures of the deposits are different as well.

5 CONCLUSION

(1) There are many differences in the calcium carbonate morphology between deposits from the experimental group and the control group. The surface micromorphology of the deposit from the experimental group seems to be the superposition of mineral layers, resulting in a scaly structure, while that in the control group had no specific characteristics. The particle sizes of the deposit from the experimental group were larger than those of the control group. The deposit from the control group was composed of nanometer-sized particles, while the other group was composed of micrometer-sized particles.

(2) The composition of the deposit from the control group was complex, containing calcium (Ca), carbon (C), oxygen (O), phosphorus (P), iron (Fe), copper (Cu), zinc (Zn), and other elements, while that from the experimental group contained fewer elements, only Ca, C, and O. Both of the deposits contained calcite. There was a preferred growth orientation for calcium carbonate in the experimental group.

(3) The decomposition temperature of the deposit from the control group was lower than that of the experimental group. The results show that the $CaCO_3$ deposits generated from the experimental group had

higher thermal stability than the deposits from the control group. Secondary metabolites produced by algae cells that interact with calcium ions may affect the arrangement of atoms in the carbonate crystal. It was estimated that the atoms were closely packed to shorten the interatomic distances. Therefore, crystals formed in this case would have higher thermal stability.

(4) There was a clear difference in weight loss between the two types of deposits at about 250°C. The weight loss from the experimental group at about 250°C was due to organic algae cell decomposition, while there was no weight loss at about 250°C for the control group. When the calcium concentration was increased in the culture medium, the number of algae cells remained after weight loss was much greater. It was believed that there were calcium crystals in the *Synechocystis* cells.

6 ACKNOWLEDGMENT

The authors express their thanks to Prof. Xuefeng LU from Qingdao Institute of Bioenergy and Bioprocess Technology for supplying the standard *Synechocystis* sp. PCC6803 strain.

References

Cacchio P, Ercole C, Cappuccio G, Lepidi A. 2003. Calcium carbonate precipitation by bacterial strains isolated from a limestone cave and from a loamy soil. *Geomicrobiol*. *J*., **20**: 85-95.

Castanier S, Le Métayer-Levrel G, Perthuisot J P. 1999. Ca-carbonates precipitation and limestone genesis—the microbiologist point of view. *Sediment*. *Geol*., **126**: 9-23.

Cölfen H. 2003. Precipitation of carbonates: recent progress in controlled production of complex shapes. *Curr*. *Opin*. *Colloid Interface Sci*., **8**: 23-31.

de Vrind-de Jong E W, de Vrind J P M. 1997. Algal deposition of carbonates and silicates. *In*: Banfield J F, Nealson K H eds. Geomicrobiology: Interactions Between Microbes and Minerals, 35. Mineralogical Society of America, Washington, DC. p.267-307.

Dittrich M, Kurz P, Wehrli B. 2004. The role of autotrophic picocyanobacteria in calcite precipitation in an oligotrophic lake. *Geomicrobiol*. *J*., **21**: 45-53.

Dittrich M, Muller B, Mavrocordatos D, Wehrli B. 2003. Induced calcite precipitation by cyanobacterium Synechococcus. *Acta Hydrochim*. *Hydrobiol*., **31**: 162-169.

Fujita Y, Ferris F G, Lawson R D, Colwell F S, Smith R W. 2000. Calcium carbonate precipitation by ureolytic subsurface bacteria. *Geomicrobiol*. *J*., **17**: 305-318.

Hammes F, Boon N, de Villiers J, Verstraete W, Siciliano S D. 2003. Strain-specific ureolytic microbial calcium carbonate precipitation. *Appl*. *Environ*. *Microbiol*., **69**: 4 901-4 909.

Hammes F, Verstraete W. 2002. Key roles of pH and calcium metabolism in microbial carbonate precipitation. *Rev*. *Environ*. *Sci*. *Biotechnol*., **1**: 3-7.

Han Z Z, Yan H X, Zhou S X, Zhao H, Zhang Y, Zhang N N, Yao C K, Zhao L, Han C Y. 2013. Precipitation of calcite induced by Synechocystis sp. PCC6803. *World J*. *Microbiol*. *Biotechnol*., http://dx.doi.org/10.1007/s11274-013-1341-1.

Kimura T, Koga N. 2011. Thermal dehydration of monohydrocalcite: overall kinetics and physico-geometrical mechanisms. *J. Phys. Chem. A*, **115**: 10 491-10 501.

Lee B D, Apel W A, Walton M R. 2006. Calcium carbonate formation by *Synechococcus* sp. strain PCC8806 and *Synechococcus* sp. strain PCC8807. *Bioresour*. *Technol*., **97**: 2 427-2 434.

Liu Y Y, Jiang J, Gao M R, Yu B, Mao L B, Yu S H. 2013. Phase transformation of magnesium amorphous calcium carbonate (Mg-ACC) in a binary solution of ethanol and water. *Cryst. Growth Des*., **13**: 59-65.

Manoli F, Dalas E. 2000. Spontaneous precipitation of calcium carbonate in the presence of chondroitin sulfate. *J*. *Cryst*. *Growth*, **217**: 416-421.

Milliman J D, Troy P J, Balch W M, Adams A K, Li Y H, Mackenzie F T. 1999. Biologically mediated dissolution of calcium carbonate above the chemical lysocline? *Deep-Sea Res*., **46**: 1 653-1 669.

Ren D N, Feng Q L, Bourrat X. 2011. Effects of additives and templates on calcium carbonate mineralization in vitro. *Chin*. *J*. *Oceanol*. *Limnol*., **42**: 228-245.

Rippka R, Deruelles J, Waterbury J, Herdman M, Stanier R. 1979. Generic assignments, strain histories and properties of pure cultures of cyanobacteria. *J*. *Gen*. *Microbiol*., **111**: 1-61.

Spanos N, Koutsoukos P G. 1998. The transformation of vaterite to calcite: effect of the conditions of the solution in contact with the mineral phase. *J*. *Cryst*. *Growth*, **191**: 783-90.

Tong H, Ma W T, Wang L L, Wan P, Hu J M, Cao L X. 2004. Control over the crystal phase, shape, size and aggregation of calcium carbonate via an L-aspartic acid inducing process. *Biomaterials*, **25**: 3 923-3 929.

Yeager C M, Milliken C E, Bagwell C E, Staples L, Berseth P A, Sessions H T. 2011. Evaluation of experimental conditions that influence hydrogen production among heterocystous Cyanobacteria. *Int*. *J*. *Hydrogen Energy*, **36**: 7 487-7 499.